Calcif Tissue Int (2015) 96:541–551
DOI 10.1007/s00223-015-9975-7

ORIGINAL RESEARCH

The Effects of Atorvastatin on the Prevention of Osteoporosis and Dyslipidemia in the High-Fat-Fed Ovariectomized Rats

Sien Lin · Jianping Huang · Ziwei Fu · Yanlong Liang · Haiyou Wu · Liangliang Xu · Yuxin Sun · Wayne Y. W. Lee · Tie Wu · Ling Qin · Liao Cui · Gang Li

Received: 2 December 2014 / Accepted: 25 February 2015 / Published online: 27 March 2015

Abstract Previous studies reported that statins showed positive effects on bone in both human and animal models. This study aimed to investigate the effects of atorvastatin on the prevention of osteoporosis and dyslipidemia in ovariectomized rats fed with high-fat emulsion. The 3-month-old female rats were subjected to either sham operations ($n = 8$) or ovariectomized operations (OVX, $n = 24$). The OVX rats were orally administered deionized water ($n = 8$) or standardized high-fat emulsion without ($n = 8$) or with atorvastatin ($n = 8$). All rats were injected twice with calcein before sacrificed for the purpose of double in vivo labeling. After 12 weeks, all rats were sacrificed under anesthesia. Biochemistry, histomorphometry, mechanical test, micro-computed tomography analysis, mechanical test, histology, and component analysis were performed. We found that high-fat emulsion significantly decreased body weight, bone formation, collagen content of bone, and bone biomechanics, while increased blood, liver, and bone marrow lipids. Atorvastatin treatment prevented dyslipidemia, reversed hepatic steatosis, optimized composition of bone, and improved bone mechanical properties. The current study provided further evidence that atorvastatin might be useful for the treatment of osteoporotic patients with dyslipidemia.

Keywords Ovariectomy · Osteoporosis · Dyslipidemia · Rat · Atorvastatin

Sien Lin and Jianping Huang have contributed equally to this study.

S. Lin · Z. Fu · Y. Liang · H. Wu · T. Wu · L. Cui (✉)
Department of Pharmacology, Guangdong Key Laboratory for Research and Development of Natural Drugs, Guangdong Medical College, Zhanjiang 524023, Guangdong, China
e-mail: cuiliao@163.com

S. Lin · L. Xu · Y. Sun · W. Y. W. Lee · L. Qin · G. Li (✉)
Department of Orthopaedics and Traumatology and Li Ka Shing Institute of Health Sciences, Faculty of Medicine, Prince of Wales Hospital, The Chinese University of Hong Kong, Shatin, Hong Kong, SAR, China
e-mail: gangli@ort.cuhk.edu.hk; gangli@cuhk.edu.hk

S. Lin · W. Y. W. Lee · G. Li
The CUHK-ACC Space Medicine Centre on Health Maintenance of Musculoskeletal System, Shenzhen Research Institute, The Chinese University of Hong Kong, Shenzhen, Guangdong, China

J. Huang
Department of Stomatology, Guangdong Medical College, Zhanjiang, Guangdong, China

W. Y. W. Lee · G. Li
MOE Key Laboratory of Regenerative Medicine, School of Biomedical Sciences, The Chinese University of Hong Kong, Shatin, Hong Kong, China

Introduction

The incidence of osteoporosis-related fractures in China is increasing dramatically [1]. Cooper et al. estimated that 51 % of the world's hip fractures would occur in Asia by 2050 due to a large aging population [2]. However, apart from aging, there are still some other factors contributed to the osteoporosis-related fracture, such as nutrition, especially high-fat diets [3]. Currently, fast food culture and globalization have taken over during the increasing urbanization in China. Dyslipidemia due to high-fat diet is also highly prevalent in postmenopausal women. There were rare data to show the effect on the osteoporosis with dyslipidemia with current treatment. However, bisphosphonates and statins were regarded as the first-line drugs for anti-osteoporosis and anti-dyslipidemia in clinical settings, respectively.

Certain bisphosphonates (i.e., nitrogen-containing bisphosphonates) act predominantly to decrease bone resorption by inhibiting activation of farnesyl diphosphate synthase in the mevalonate pathway [4, 5]. Interestingly, 3-hydroxy-3-methylglutarylcoenzyme A (HMG-CoA) reductase inhibitors statins which inhibit the same pathway and lower the blood cholesterol level have been shown to inhibit osteoclastic bone resorption in a fashion similar to bisphosphonates [6, 7]. The question is whether statins could attenuate both dyslipidemia and osteoporosis in the same animal model. Could we kill two birds with one stone?

Bisphosphonates are the most widely used anti-resorptive agents because they are effective and inexpensive. Although these agents reduce the incidence of fractures, they do not increase bone formation. Furthermore, long-term use of bisphosphonates showed some adverse effects, such as subtrochanteric femoral fractures, osteonecrosis of the jaw, esophageal irritation, etc., which had negative impact on patients' compliance [8].

Apart from the inhibitory effect on osteoclasts differentiation [9], statins also activated osteoblasts by inducing synthesis of bone morphogenetic protein-2 [10, 11]. Similar results were also reported in clinical studies showing beneficial effects on blood lipids disorders, osteoporosis, and fracture prevention [12–18]. Meta-analysis of clinical studies showed that statins possessed positive effect on bone mineral density (BMD) in multiple bone sites and reduced hip fracture risk [19, 20]. However, the effect of statin on bone turnover was still controversial in other clinical trial on postmenopausal women with modest elevations of low-density lipoprotein (LDL) cholesterol [21]. Hence, it is worthy to investigate the effects of statins on the prevention of osteoporosis and dyslipidemia in controlled animal model.

This study aimed to investigate the effects and the underlying mechanisms of statins on the prevention of osteoporosis and dyslipidemia in ovariectomized rats fed with high-fat emulsion. Body weight observation, biochemistry, histomorphometry, mechanical test, micro-computed tomography (micro-CT), histology, and component analysis were performed. Atorvastatin (AT) was used in current study because it is the most widely prescribed statins in clinics. The routine clinical dosage of AT is range from 10 to 80 mg each day. The highest dosage 80 mg was chosen in this study, which was equivalent to 3.6 mg/kg in rats [22, 23].

Materials and Methods

Animals and Treatments

This study was carried out in strict accordance with the recommendations in the Guide for the Care and Use of Laboratory Animals of Guangdong Laboratory Animal Monitoring Institute, the National Laboratory Animal Monitoring Institute of China. All procedures performed in this studies involving animals were in accordance with the ethical standards of the Academic Committee on the Ethics of Animal Experiments of the Guangdong Medical College. 3-month-old Sprague–Dawley female rats were acclimated to local vivarium conditions (temperature 24–26 °C, humidity 67 %) and allowed free access to water and diets containing 1.11 % calcium, 0.74 % phosphorus. All rats received subcutaneous injections with calcein (10 mg/kg, Sigma-Aldrich, St. Louis, MO, USA) on days 14, days 13, days 4 and 3 before sacrifice.

The rats were subjected to either sham operation ($n = 8$) or bilaterally ovariectomized operation ($n = 24$) as previously described [25]. After a 3-day postoperative recovery period, both the sham-operated rats (CON, $n = 8$) and 8 OVX rats (OVX, $n = 8$) were orally administered deionized water. The remaining OVX rats ($n = 16$) were orally administered 5 ml/kg/day high-fat emulsion containing 50 % lard oil (local fresh market), 10 % cholesterol (China Xinxing Chemical Institute, Shanghai, China), 2 % sodium cholate (China Xinxing Chemical Institute, Shanghai, China), and 1 % propylthiouracil (Jinghua Pharmaceutical Co., Nantong, Jiangsu, China) without addition ($n = 8$, OVX + fat) or with 3.6 mg/kg AT (Pfizer Pharmaceutical Co., Shanghai, China; $n = 8$, OVX + fat + At). All the rats were treated for 12 weeks post operation.

Sample Collection and Applications

Rats were weighed weekly. At the endpoint, the rats were sacrificed by cardiac puncture under anesthesia using overdose of sodium pentobarbitone. The serum was collected for biochemical assays. The uteri and livers were isolated, weighed, and normalized by body weights. The 4th lumbar vertebras (LV4) were dissected for measurement of trabecular micro-CT analysis. The left proximal tibial metaphysis (PTM) and left tibial shaft (TS) were performed in undecalcified sections for the analysis of bone histomorphometry. The 6th lumbar vertebras (LV6) were performed in decalcified sections for the measurement of fat tissue in bone marrow. The right femora and 5th lumbar vertebras (LV5) were dissected for measurement of biomechanics. The uteri, livers, and thoracic aortas were collected for histological analysis.

Serum Markers Assays

Blood was collected in specimen tubes and kept at 25 °C for 40–50 min in a vertical position until complete clotting. And then the serum was separated by centrifuging at $1000 \times g$ for 10 min and stored at −80 °C for biochemical

markers assays. Serum levels of total cholesterol (TC), triglyceride (TG), LDL cholesterol, and high-density lipoprotein (HDL) cholesterol were determined by colorimetric assays based on the enzyme-driven reaction with commercial kits (Nanjing Jiancheng Biological Bioengineering, Nanjing, Jiangsu, China) using ELX800 Microplate Reader (Bio-Tek Instruments, Winooski, VT, USA) according to the protocols attached.

Bone Histomorphometry

The left PTM and TS were collected and trimmed with IsoMet® precision bone saw (Buehler, Lake Bluff, IL, USA), and then were fixed in 10 % buffered formalin for 24 h, followed by gradient alcohol dehydration, xylene defatting, and embedded in methyl methacrylate. The frontal PTM tissue was cut into 9- and 5-μm-thick sections with the RM2155 hard tissue microtome (Leica, Wetzlar, Germany), respectively. The unstained 9-μm sections were used for dynamic histomorphometric analysis. The 5-μm sections were stained with trichrome masson goldner for static histomorphometric measurements. TS was cut using IsoMet® precision bone saw, and sections were mounted on plastic slides, ground, and polished for histomorphometry. A semi-automatic digitizing image analysis system (OsteoMetrics, Atlanta, GA, USA) was used for quantitative bone histomorphometry measurements [24–26].

The measurement region of PTM was cancellous bone between 1 and 4 mm distal to the growth plate-epiphyseal junction. The measurement region of interest for cortical bone analyses included the cross section of mid-tibial shaft. The quantitative analysis was performed on each sample, with one section each. Dynamic histomorphometry and bone cell measurement were performed under magnifications of ×100 and ×400, respectively. The histomorphometric measurements were done on the cancellous (Cn) and cortical (Ct) bone. The abbreviations of the bone histomorphometric parameters used were recommended by the ASBMR Histomorphometric Nomenclature Committee [27]. All measured thicknesses (except cortical thickness) were multiplied by π/4. Structural parameters were tissue volume (TV), bone volume (BV), marrow volume (Ma.V), bone surface (BS), cortical thickness (Ct.Th), marrow diameter (Ma.Dm), periosteal surface (Ps.S), and endocortical surface (Ec.S). Dynamic measurement parameters were single-labeled surface (sL.S), double-labeled surface (dL.S), and label thickness (L.Th). Bone formation or resorption were assessed with measurements of osteoblast surfaces (Ob.S/BS) or osteoclast surface (Oc.S/BS). The mineral apposition rate (MAR), the ratio of mineralizing surface to bone surface (MS/BS, calculated as double plus half of single-labeled surfaces), bone formation rate per unit of bone surface (BFR/BS), and bone formation rate per unit of bone volume (BFR/BV) were analyzed on unstained sections under ultraviolet light.

Biomechanical Test

The right femora and LV5s were used to determine the bone mechanical properties through three-point bending or compression test using material testing machine (H25KS Hounsfield Test Equipment Ltd., UK) with 25 N load cell. Before mechanical testing, the femora and LV5s were taken out from the freezer and thawed overnight at air-conditioned room temperature. The vertebral bodies were isolated from the intervertebral disks and the vertebral pedicles. Our specimen preparation assured parallel superior and inferior surfaces of the vertebral body. The femora were positioned horizontally to the base with the anterior surface upward, and centered on the supports with 10 mm apart. The LV5s were positioned vertically to the base. Load was applied on the mid-shaft of femur or LV5 constantly with the displacement rate of 5 mm/min. After failure, the load versus displacement curves were recorded. The maximum load and the energy to failure (energy resorption) were calculated using built-in software (QMAT Professional; Tinius Olsen, Inc. Horsham, PA, USA).

Micro-computed Tomography (micro-CT) Scanning

The LV4s were scanned using a desktop preclinical specimen micro-CT (μCT-40, Scanco Medical, Bassersdorf, Switzerland). Briefly, the vertebral bodies were aligned perpendicularly to the scanning axis for a total scanning length of 6.0 mm at custom isotropic resolution of 8-μm isometric voxel size with a voltage of 70 kV p and a current of 114 μA. Three-dimensional (3D) reconstructions of mineralized tissues were performed by an application of a global threshold (211 mg hydroxyapatite/cm^3), and a Gaussian filter (sigma = 0.8, support = 2) was used to suppress noise. A volume of interest (VOI) containing only trabecular bone within the vertebral body extracted from the cortical bone with 1.80-mm thick (150 slices) was acquired 1.0–1.2 mm from both cranial and caudal growth plate-metaphyseal junctions. The three-dimensional reconstructed images were used directly to quantify microarchitecture, and the morphometric parameters including bone volume fraction (BV/TV), trabecular number (Tb.N, 1/mm), trabecular thickness (Tb.Th, mm), trabecular separation (Tb.Sp, mm), structure model index (SMI, 1), and connective density (Conn.D, 1/mm^3) were calculated with the image analysis program of the micro-CT workstation (Image Processing Language v4.29d, Scanco Medical, Switzerland) [28].

Histological Examination

The bone marrow cavity of LV6 was exposed and decalcified at room temperature in 10 % buffered EDTA for 5 weeks. Then the bone samples, uteri, livers, and thoracic aortas were dehydrated and paraffin embedded. 5-μm-thick sections were prepared then followed with hematoxylin and eosin staining (H&E) as previously described [26]. Five fields under a magnification of ×100 were randomly selected for the evaluation of each sample; the mean value of all fields measured for each animal was taken for statistical analysis. Percentages of fat area in bone marrow (fat cells area divided by tissue area in the examined regions) and liver were evaluated with imaging process software, Image-Pro-Plus 6.0 (Media Cybernetics Inc., Bethesda, MD, USA) [26]. The thicknesses of uteri and tunica media of thoracic aortas were also measured with the semi-automatic digitizing image analysis system (OsteoMetrics, Atlanta, GA, USA).

Sample Digestion and Component Analysis

After subjected to mechanical test, the femora were digested and subjected to component analysis as previously report [29]. Briefly, samples were weighed before and after placing at 80 °C oven for 72 h. Then the desiccant bones were digested with 6 mol/l hydrochloric acid in 10-ml ampoule bottles at 108 °C oven for 24 h. Calcium and phosphorus in bone samples were determined by Inductively Coupled Plasma emission spectrometer (ICP-IRIS/AP, Thermo Jarrell Ash, Franklin, MA, USA). Instrument operating conditions applied for calcium and phosphorus determined were as follows: gas (plasma) 24 l/min, gas flow (auxiliary) 0.5 l/min, RF power 1150 W, sample aspiration rate 1.48 ml/min, and pressure 30 psi. Standard calcium (Sigma-Aldrich, St. Louis, MO, USA) and phosphorus (Sigma-Aldrich, St. Louis, MO, USA) at concentrations of 10 and 50 μg/ml were taken as controls, respectively. Hydroxyproline in bone digestive solution was determined by colorimetric (550 nm) assays according to the manufacturer's instructions (Nanjing Jiancheng Biological Bioengineering, Nanjing, Jiangsu, China).

Statistical Analysis

Data were presented as mean ± SD, and analyzed using SPSS16.0 software for Windows (SPSS, Chicago, IL, US). The statistical differences among groups were analyzed by ANOVA with post hoc Turkey's HSD. Probabilities (P) less than 0.05 were considered significant.

Results

Body and Organ Weight Changes

As shown in Fig. 1a, mean body weight of the OVX rats increased ($P < 0.01$) at the endpoint. High-fat feeding significantly decreased the body weight ($P < 0.01$) of the OVX rats, while AT could only slightly increase body weight ($P > 0.05$) of the OVX rats fed with high-fat emulsion (Fig. 1a).

Results (Fig. 1b, c) showed that high-fat feeding also significantly increased liver weight ($P < 0.01$) of the OVX rats, while AT significantly decreased liver weight ($P < 0.01$). There was no effect on the uterus weight in the high-fat feeding animals treated with or without AT (Fig. 1c).

Serum Markers

There was no significant change in the serum lipids (TG, TC, LDL, and HDL) after ovariectomy (Fig. 2). However, high-fat feeding significantly increased serum TC and LDL level and decreased serum TG level (Fig. 2). AT significantly decreased TC level and increased HDL level in the OVX rats fed with high-fat emulsion (Fig. 2).

Microarchitecture of Trabecular Bone

Trabecular microarchitecture of 4th vertebral bodies was analyzed by micro-CT, and the representative 3D images are shown in Fig. 3a. The quantitative data showed that BV/TV ($P < 0.01$) and Tb.N ($P < 0.01$) were significantly decreased, while Tb.Sp ($P < 0.01$) and SMI ($P < 0.01$) were significantly increased in the OVX rats (Fig. 3). Except for the changes in Con.D, Tb.Sp, and SMI, no significant change in BV/TV, Tb.N and Tb.Th was found in the OVX rats fed with high-fat emulsion (Fig. 3). When compared with OVX rats treated with deionized water, AT significantly increased BV/TV ($P < 0.05$), Tb.N ($P < 0.05$), and Con.D ($P < 0.05$), while decreased Tb.Sp ($P < 0.01$) and SMI ($P < 0.01$) (Fig. 3). Although there was an increasing trend in BV/TV, Tb.N, Tb.Th, and Con.D with a decreasing trend in Tb.Sp and SMI in the AT-treated rats, there was no significant difference in the microarchitecture between the high-fat feeding animals treated with water or AT (Fig. 3).

Bone Histomorphometry

Histomorphometric data showed that MS/BS ($P < 0.05$), BFR/BV ($P < 0.05$), and Oc.S/BS ($P < 0.05$) were significantly increased in the OVX rats versus sham-operated

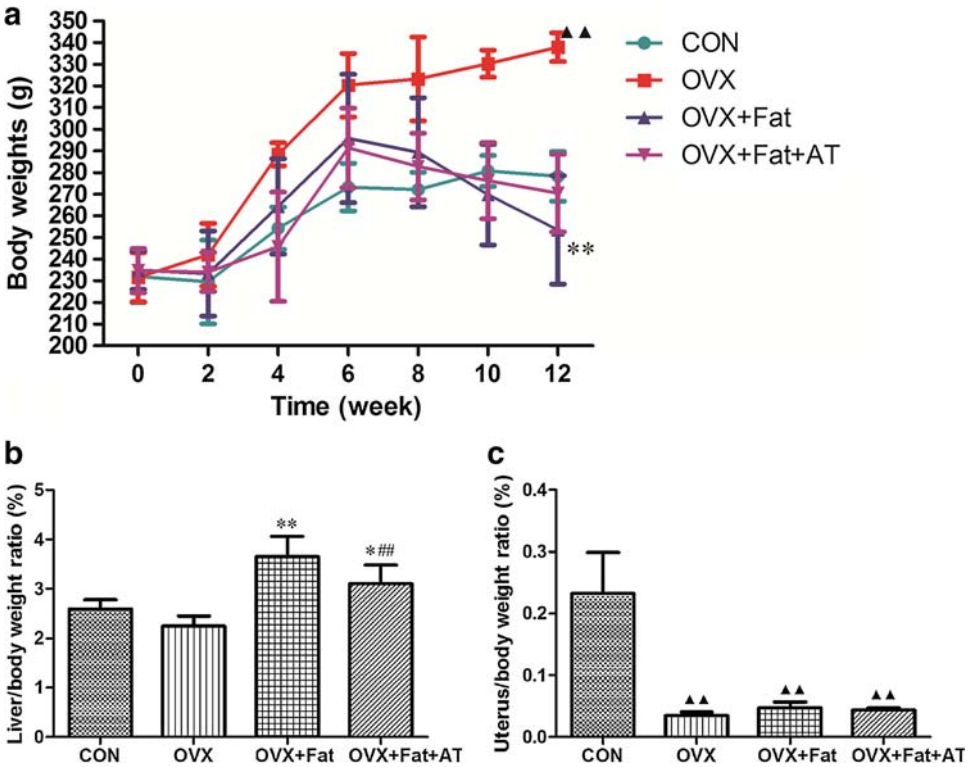

Fig. 1 Body weight measurements (**a**) during the experimental period and endpoint liver (**b**) and uterus weight:body weight ratio (**c**) from sham-operated controls (CON), ovariectomized rats treated with deionized water (OVX) or high-fat emulsion (OVX + fat) without addition or with atorvastatin (OVX + fat + AT). ▲▲$P < 0.01$ versus CON; **$P < 0.01$, versus OVX; ##$P < 0.01$ versus OVX + fat

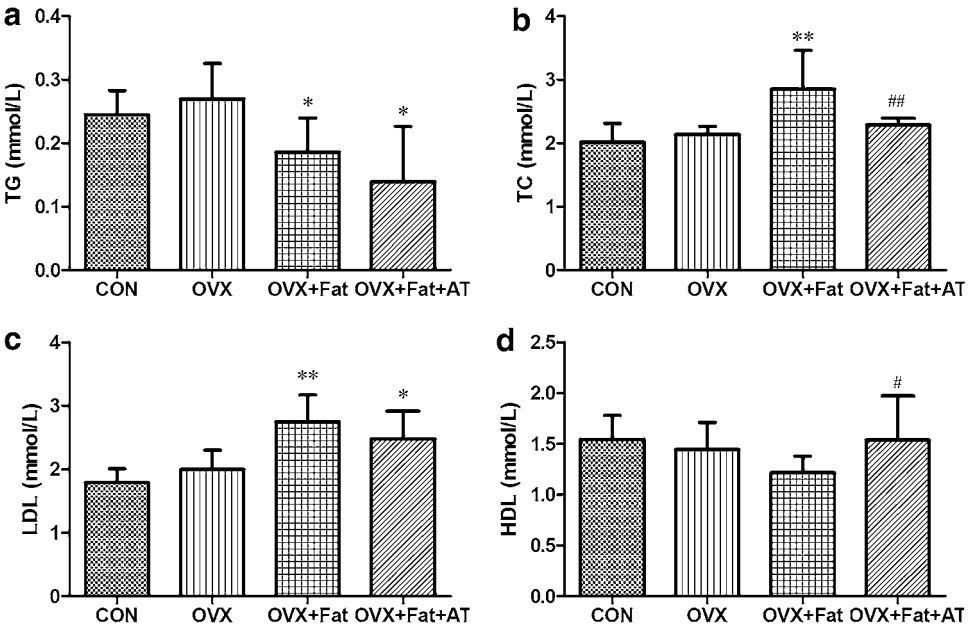

Fig. 2 Endpoint levels of serum biochemical markers (**a** TG, **b** TC, **c** LDL, **d** HDL).*$P < 0.05$, **$P < 0.01$, versus OVX; #$P < 0.05$, ##$P < 0.01$ versus OVX + fat

controls (Fig. 4; Table 1). High-fat feeding significantly decreased MS/BS ($P < 0.01$), MAR ($P < 0.05$), BFR/BS ($P < 0.05$), BFR/BV ($P < 0.05$), and Ob.S/BS ($P < 0.05$) (Fig. 4; Table 1). AT treatment significantly increased MS/BS ($P < 0.01$), while slightly increased MAR, BFR/BS, BFR/BV, Ob.S/BS, and decreased Oc.S/BS without statistical significant difference (Fig. 4; Table 1). For the cortical bone, dynamic histomorphometric data showed that high-fat feeding significantly decreased Ps-MS/BS ($P < 0.05$), Ps-MAR ($P < 0.05$), and Ec-MS/BS ($P < 0.05$) (Fig. 4; Table 2). Our results also showed that AT treatment significantly increased Ps-MS/BS ($P < 0.05$) and Ec-MS/BS ($P < 0.05$) (Fig. 4; Table 2).

Bone Biomechanics

At the endpoint, high-fat feeding significantly decreased maximum load ($P < 0.01$) and energy absorption ($P < 0.05$)

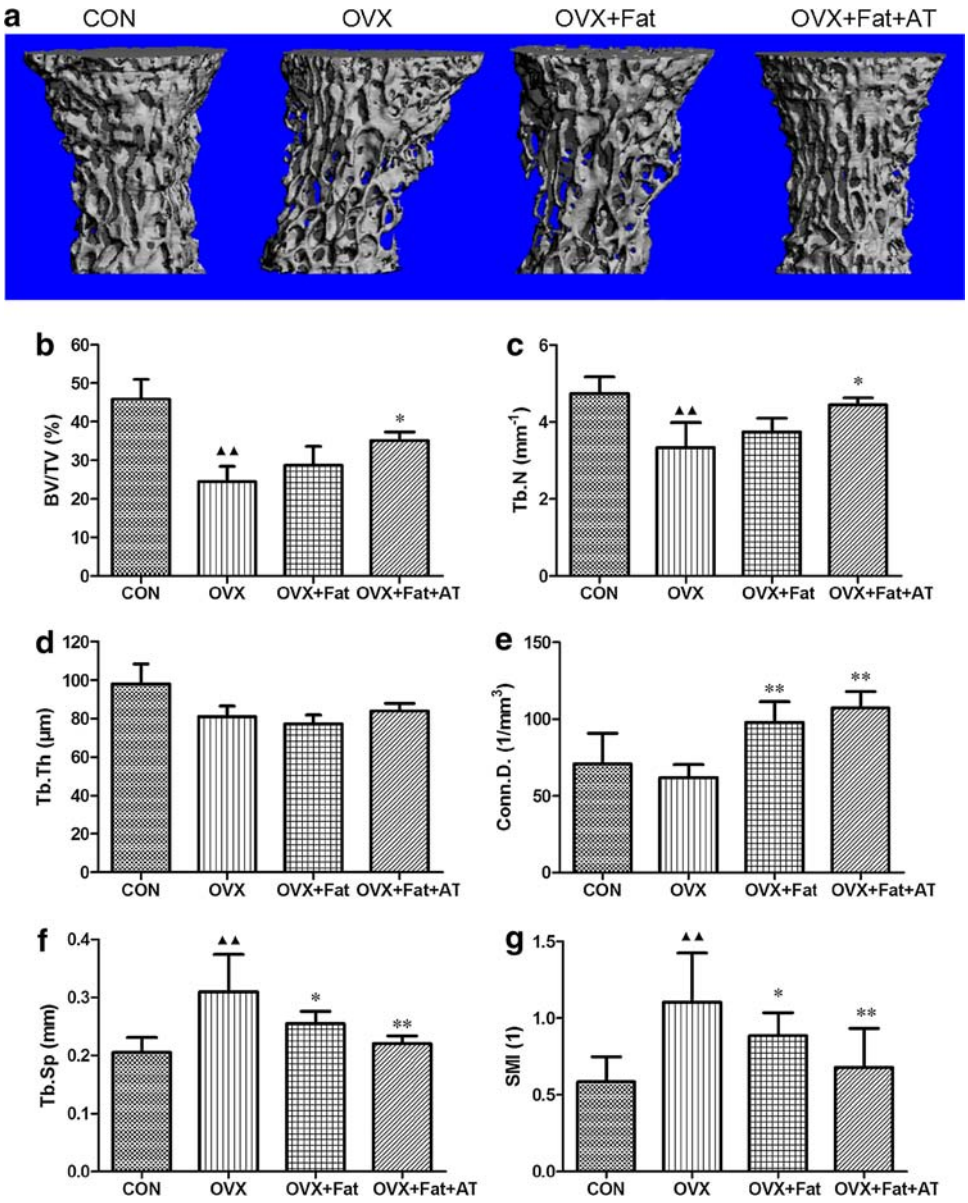

Fig. 3 The representative images (**a**) and trabecular microarchitecture (**b** BV/TV, **c** Tb.N, **d** Tb.Th, **e** Conn.D, **f** Tb.Sp, **g** SMI) of LV4. ▲▲$P < 0.01$ versus CON; *$P < 0.05$, **$P < 0.01$, versus OVX

in the femora and decreased maximum load ($P < 0.01$) and Young's modulus ($P < 0.05$) in the LV5s (Fig. 5). AT significantly increased the maximum load ($P < 0.05$) and energy absorption ($P < 0.05$) in the femora and maximum load ($P < 0.05$) in the LV5s (Fig. 5).

Histological Analysis

Histological data showed that fat tissue area in the marrow cavity of calcified LV6 was significantly increased and hepatic steatosis also happened in the OVX rats fed with high-fat emulsion (Fig. 6). This lipid accumulation in bone and liver could be reversed by the treatment of AT (Fig. 6). Uterus atrophy was observed in the OVX rats, while there was no effect on the uterus thickness in the high-fat feeding animals treated with or without AT (Fig. 6). There was no pathological change in the thoracic aorta of all the animals (Fig. 6).

Chemical Compositions of Bone

As shown in Table 3, the contents of calcium and hydroxyproline were significantly decreased ($P < 0.05$ and $P < 0.05$) in the OVX rats. High-fat feeding significantly decreased the contents of phosphorus ($P < 0.05$) and hydroxyproline ($P < 0.05$). AT significantly increased the content of hydroxyproline ($P < 0.05$).

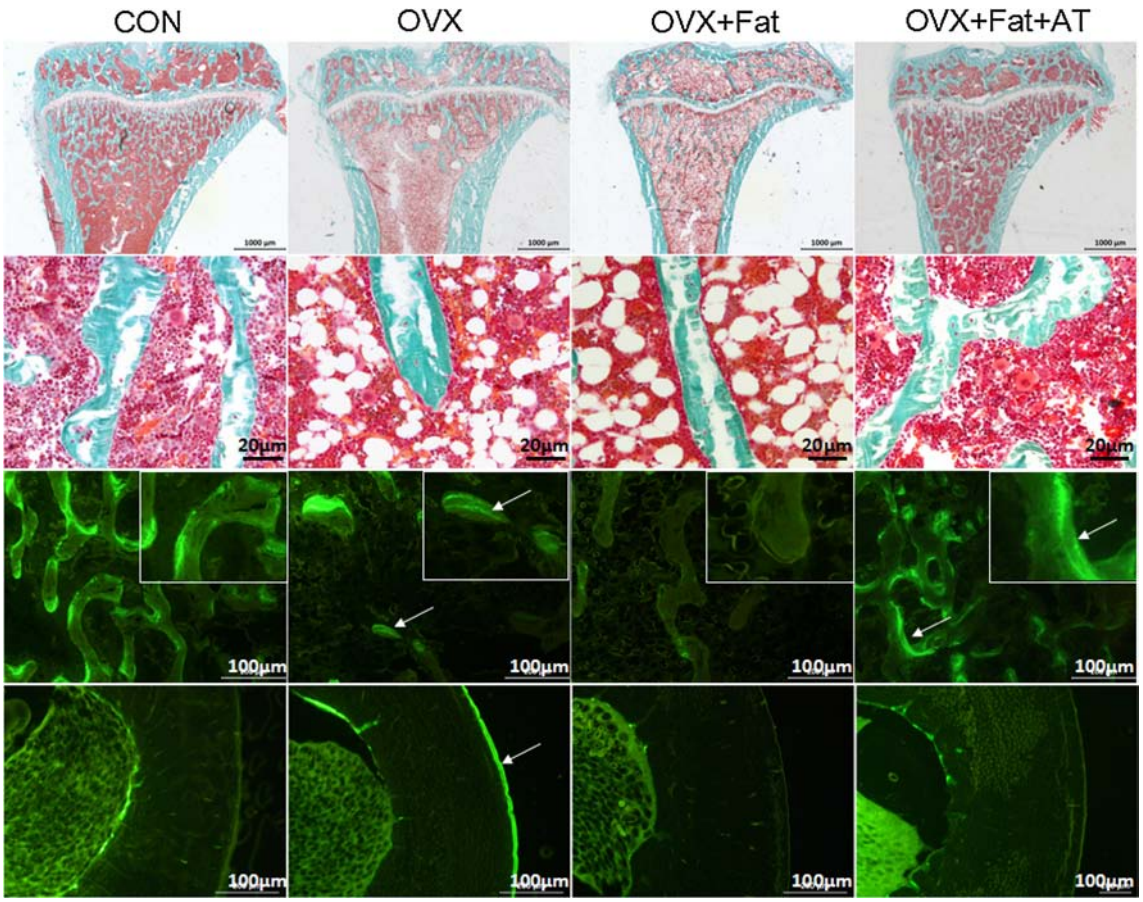

Fig. 4 Histomorphometric images of proximal tibial metaphyses (PTM) and tibial shaft (TS) structure and mineral bone formation. *Arrows* point to the double calcein labels. Quantitative measurements of histomorphometric parameters of PTM and TS are shown in Tables 1 and 2, respectively. (*Upper two panels*, Goldner's Trichrome stain; *lower two panels*, fluorescent images of trabecular bone and cortical bone)

Table 1 Histomorphometric results of proximal tibial metaphysis cancellous bone dynamic parameters, osteoblast, and osteoclast surface

Group	MS/BS (%)	MAR (μm/d)	BFR/BS (μm/d × 100)	BFR/BV (%/year)	Ob.S/BS (%)	Oc.S/BS (%)
CON	21.3 ± 4.1	1.0 ± 0.21	18.5 ± 7.3	231.3 ± 52.4	1.8 ± 0.4	0.32 ± 0.13
OVX	34.3 ± 7.7▲	1.4 ± 0.40	26.4 ± 6.6	346.4 ± 141.7▲	2.5 ± 0.7	0.54 ± 0.27▲
OVX + fat	12.2 ± 5.1**	0.7 ± 0.25*	12.2 ± 4.8*	185.9 ± 94.2*	1.0 ± 0.3*	0.45 ± 0.25
OVX + fat + At	19.5 ± 3.9#	1.1 ± 0.32	17.9 ± 6.7	210.7 ± 80.1	1.5 ± 0.5	0.39 ± 0.17*

▲ $P < 0.05$ versus CON; * $P < 0.05$, ** $P < 0.01$ versus OVX; # $P < 0.05$ versus (OVX + fat)

Discussion

We report here that low body weight was observed in the high-fat feeding OVX rats. This result might be due to the loss of appetite caused by oral administration of high-fat emulsion. And the administration of fat in this study is oral gavage, which is considered to be a compulsive way. It has been well established that the interaction of dietary fat with the small intestine induces potent effects on gastrointestinal function that contribute to the suppression of hunger and energy intake [30].

However, dyslipidemia including high TC and LDL level and low TG level was presented in addition to lipid accumulation in the livers in high-fat feeding animals. Even though dyslipidemia was found in the high-fat feeding rats, atherosclerosis was not detected in the thoracic aortas. A decrease in serum TG and hepatic steatosis was also previously observed in high-fat feeding OVX rats,

Table 2 Histomorphometric results of cortical bone of tibia shaft (TS) dynamic parameters

Group	Ps-MS/BS (%)	Ps-MAR (μm/d)	Ps-BFR/BS (μm/d × 100)	Ec-MS/BS (%)	Ec-MA (μm/d)	Ec-BFR/BS (μm/d × 100)
CON	38.7 ± 8.4	0.8 ± 0.2	373.3 ± 120.5	91.3 ± 35.7	2.6 ± 0.4	223.5 ± 96.0
OVX	52.8 ± 12.7▲	1.1 ± 0.4	382.4 ± 119.2	92.1 ± 21.7	2.7 ± 0.6	240.4 ± 89.8
OVX + fat	24.3 ± 6.9*	0.6 ± 0.2*	278.7 ± 80.5	58.9 ± 34.8*	2.1 ± 0.3	198.1 ± 76.7
OVX + fat + At	35.5 ± 7.8#	0.7 ± 0.3	323.9 ± 89.7	80.7 ± 24.4#	2.3 ± 0.5	218.9 ± 79.1

▲ $P < 0.05$ versus CON; * $P < 0.05$ versus OVX; # $P < 0.05$ versus (OVX + fat)

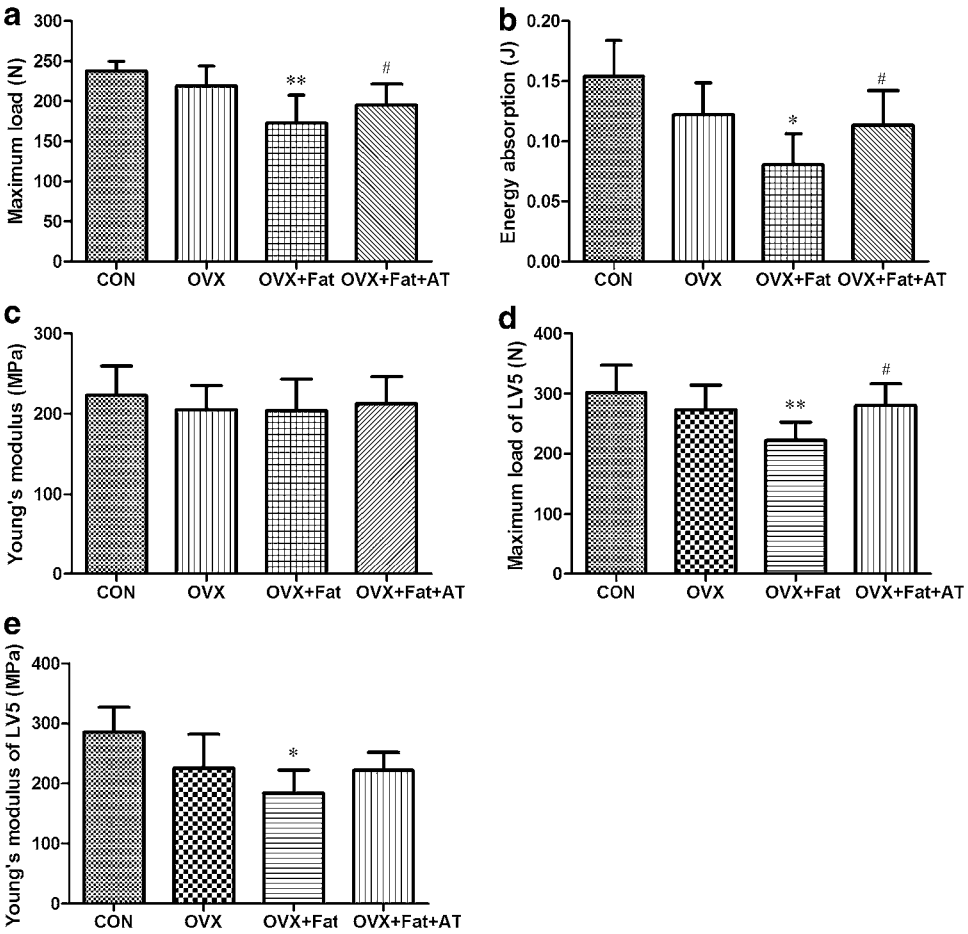

Fig. 5 Results of three-point bending test on femora (**a** Maximum load, **b** Energy absorption, **c** Young's modulus) or compressive loading test on 5th lumbar vertebral bodies (LV5) (**d** Maximum load, **e** Young's modulus). *$P < 0.05$, **$P < 0.01$, versus OVX; #$P < 0.05$ versus OVX + fat

indicating that the absence of a normal estrogenic status synergistically favors fat accumulation in liver when combined to high-fat feeding [31]. Our study, however, indicated that AT may play a role in the prevention of dyslipidemia and hepatic steatosis caused by high-fat feeding in OVX rats. The underlying mechanism of lipid metabolism regulated by statins has been fully demonstrated by previous publications, which will not be addressed in this study [32–34].

High-fat feeding and ovariectomy led to a status of low bone formation, low mechanical properties, abnormal composition of bone, and high lipid accumulation in bone marrow. However, no significant bone loss happened in these models. Although previous studies suggested that high-fat diet reduced bone mineralization, trabecular bone mass and increased bone turnover in normal animals [3, 35–37], we demonstrate that these changes would not happen in OVX animals. Current data showed that high-fat feeding did not reduce bone mass but decreased bone formation and collagen content (hydroxyproline) of bone in OVX rats, which indicated that dietary fat might not result in bone lost but changes composition of bone in OVX animals, thus reducing bone mechanical properties.

Our histomorphometric data showed that AT significantly increased mineral surface ratio (MS/BS), and slightly, but not significantly, increased MAR, BFR/BS,

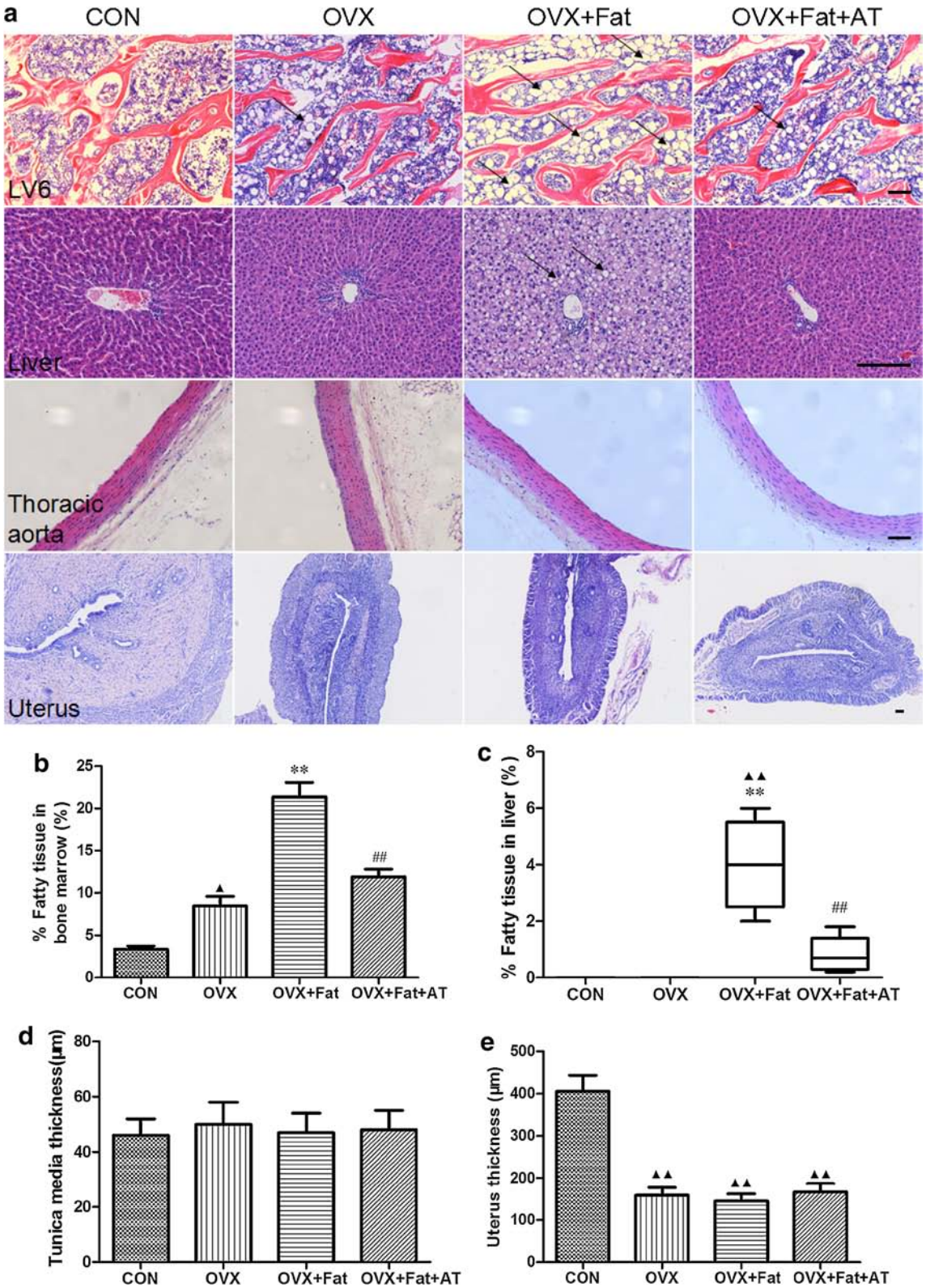

Fig. 6 The representative histological images (**a**) and quantitative data of percentage fatty tissue in liver (**b**), percentage fatty tissue in bone marrow (**c**), tunica media thickness (**d**), and uterus thickness (**e**). Hematoxylin and eosin stain. *Arrows* point to the fat tissue area. *Scale bar* = 50 μm. $^{\blacktriangle}P < 0.05$, $^{\blacktriangle\blacktriangle}P < 0.01$ versus CON; $^{**}P < 0.01$ versus OVX; $^{\#\#}P < 0.01$ versus OVX + fat

Table 3 Chemical compositions of femora determined by component analysis

Group	Calcium (mg/g)	Phosphorus (mg/g)	Hydroxyproline (mg/g)
CON	23.83 ± 2.11	12.22 ± 0.23	3.12 ± 0.24
OVX	21.34 ± 2.67▲	11.70 ± 1.39	2.36 ± 0.21▲
OVX + fat	20.57 ± 1.67	10.71 ± 1.12*	1.72 ± 0.12*
OVX + fat + At	22.10 ± 2.93	11.86 ± 0.87	2.59 ± 0.29#

▲ $P < 0.05$, versus CON; * $P < 0.05$ versus OVX; # $P < 0.05$ versus (OVX + fat)

and BFR/BV both in trabecular and cortical bone. However, there was no significant increase in Ob.S/BS or reduction in Oc.S/BS happened in the rats treated with AT, which might result in no significant increase in bone mass (BV/TV). Interestingly, AT treatment significantly improved bone maximum load both in femur and lumbar vertebra, and increased energy to failure (energy absorption) in femur. Furthermore, AT significantly increased collagen content of bone. A double-blind, placebo-controlled, dose-ranging trial has been performed to evaluate the effect of AT in 626 postmenopausal women with low-density lipoprotein cholesterol levels on osteoporosis [21]. Results revealed that the clinically relevant doses of AT that lower lipid levels had no effect on BMD or biochemical indices of bone metabolism after treated for 52 weeks [21]. This clinical trial, however, has not reported any data on the fracture risk assessment. The ability of bone to provide mechanical support and resist fracture depends on both bone structure and material composition of bone, both of which must be actively maintained in response to mechanical loading [38]. Bone is composed of type I collagen stiffened by crystals of calcium hydroxyapatite to resist deformation. An increase in content of bone calcium and collagen increases the stiffness and flexibility of bone. Our results indicated that a clinically relevant dose of AT not only decreased serum lipid levels but also promoted bone biomechanics and increased collagen content of bone in our model, which was consistent with clinical findings described above [12–18]. Although we have no evidence to show the exact mechanism of statins regulating bone metabolism, previous data indicated that statins not only activated the osteoblast function by increasing synthesis of bone morphogenetic protein-2 [10, 11], but also antagonized the osteoclasts and reduced the production of osteoclasts [39, 40].

In conclusion, our results confirmed the beneficial role of AT which acts as a double therapeutic weapon in an animal model. We revealed that AT may not only normalize cholesterol level and prevent liver lipids accumulation, but also increase bone formation and optimize composition of bone, then improve bone biomechanics. It is indicated that statin has the potential of preventing osteoporotic fracture and normalizing blood lipids in postmenopausal women. Further clinical studies are needed to determine the role of statins in the treatment of postmenopausal osteoporosis with dyslipidemia.

Acknowledgments This project was funded by Science & Technology Innovation Fund of Guangdong Medical College (No STIF201104) and Science and Technology Planning Project of Zhanjiang (No 2012C3102015). The works were also supported in part by SMART program, Lui Che Woo Institute of Innovative Medicine, Faculty of Medicine, The Chinese University of Hong Kong. We wish to thank Dr. David William Green at the University of Hong Kong for his contribution on English language editing and grammar correction of the manuscript.

Conflict of Interest Sien Lin, Jianping Huang, Ziwei Fu,Yanlong Liang, Haiyou Wu, Liangliang Xu, Yuxin Sun, Wayne YW Lee, Tie Wu, Ling Qin, Liao Cui, and Gang Li declare that they have no conflict of interest.

Human and Animal Rights and Informed Consent All animal experiments were approved by the Academic Committee on the Ethics of Animal Experiments of the Guangdong Medical College, Zhanjiang, China. Permit Number: SYXK (GUANGDONG) 2008-0007. All procedures performed in studies involving animals were in accordance with the ethical standards of Guangdong Medical College.

References

1. Xia WB, He SL, Xu L, Liu AM, Jiang Y, Li M, Wang O, Xing XP, Sun Y, Cummings SR (2012) Rapidly increasing rates of hip fracture in Beijing, China. J Bone Miner Res 27:125–129
2. Cooper C, Cole ZA, Holroyd CR, Earl SC, Harvey NC, Dennison DM, Melton LJ, Cummings SR, Kanis JA (2011) Secular trends in the incidence of hip and other osteoporotic fractures. Osteoporos Int 22:1277–1288
3. Wohl GR, Loehrke L, Watkins BA, Zernicke RF (1998) Effects of high-fat diet on mature bone mineral content, structure, and mechanical properties. Calcif Tissue Int 63:74–79
4. van Beek E, Pieterman E, Cohen L, Lowik C, Papapoulos S (1999) Farnesyl pyrophosphate synthase is the molecular target of nitrogen-containing bisphosphonates. Biochem Biophys Res Commun 264:108–111
5. Fisher JE, Rogers MJ, Halasy JM, Luckman SP, Hughes DE, Masarachia PJ, Wesolowski G, Russell RG, Rodan GA, Reszka AA (1999) Alendronate mechanism of action: geranylgeraniol, an intermediate in the mevalonate pathway, prevents inhibition of

osteoclast formation, bone resorption, and kinase activation in vitro. Proc Natl Acad Sci USA 96:133–138
6. Halcox JP, Deanfield JE (2004) Beyond the laboratory: clinical implications for statin pleiotropy. Circulation 109:II42–II48
7. Maritz FJ, Conradie MM, Hulley PA, Gopal R, Hough S (2001) Effect of statins on bone mineral density and bone histomorphometry in rodents. Arterioscler Thromb Vasc Biol 21:1636–1641
8. Drake Matthew T, Clarke Bart L, Khosla Sundeep (2008) Bisphosphonates: mechanism of action and role in clinical practice. Mayo Clin Proc 83:1032–1045
9. Grasser WA, Baumann AP, Petras SF, Harwood HJ Jr, Devalaraja R, Renkiewicz R, Baragi V, Thompson DD, Paraklar VM (2003) Regulation of osteoclast differentiation by statins. J Musculoskelet Neuronal Interact 3:53–62
10. Chen PY, Sun JS, Tsuang YH, Chen MH, Weng PW, Lin FH (2010) Simvastatin promotes osteoblast viability and differentiation via Ras/Smad/Erk/BMP-2 signaling pathway. Nutr Resm 30:191–199
11. Maeda T, Matsunuma A, Kawane T, Horiuchi N (2001) Simvastatin promotes osteoblast differentiation and mineralization in MC3T3-E1 cells. Biochem Biophys Res Commun 280:874–877
12. Chan KA, Andrade SE, Boles M, Buist DS, Chase GA, Donahue JG, Goodman MJ, Gurwitz JH, LaCroix AZ, Platt R (2000) Inhibitors of hydroxymethylglutaryl-coenzyme A reductase and risk of fracture among older women. Lancet 355:2185–2188
13. Uysal AR, Delibasi T, Erdogan MF, Kamel N, Baskal N, Tonyukuk V, Corapcioglu D, Güllü S, Erdogan G (2007) Effect of simvastatin use on bone mineral density in women with type 2 diabetes. Endocr Pract 13:114–116
14. Majima T, Komatsu Y, Fukao A, Ninomiya K, Matsumura T, Nakao K (2007) Short term effects of atorvastatin on bone turnover in male patients with hypercholesterolemia. Endocr J 54:145–151
15. Majima T, Shimatsu A, Komatsu Y, Satoh N, Fukao A, Ninomiya K, Matsumura T, Nakao K (2007) Shortterm effects of pitavastatin on biochemical markers of bone turnover in patients with hypercholesterolemia. Intern Med 46:1967–1973
16. Safaei H, Janghorbani M, Aminorroaya A, Amini M (2007) Lovastatin effects on bone mineral density in postmenopausal women with type 2 diabetes mellitus. Acta Diabetol 44:76–82
17. Schoofs MW, Sturkenboom MC, van der Klift M, Hofman A, Pols HA, Stricker BH (2004) HMG-CoA reductase inhibitors and the risk of vertebral fracture. J Bone Miner Res 19:1525–1530
18. Rejnmark L, Olsen ML, Johnsen SP, Vestergaard P, Sorensen HT, Mosekildeb L (2004) Hip fracture risk in statin users: a population-based Danish case-control study. Osteoporos Int 15:452–458
19. Hatzigeorgiou C, Jackson JL (2005) Hydroxymethylglutaryl-coenzyme A reductase inhibitors and osteoporosis: a meta-analysis. Osteoporos Int 16:990–998
20. Uzzan B, Cohen R, Nicolas P, Cucherat M, Perret GY (2007) Effects of statins on bone mineral density: a meta-analysis of clinical studies. Bone 40:1581–1587
21. Bone HG, Kiel DP, Lindsay RS, Lewiecki EM, Bolognese MA, Leary ET, Lowe W, McClung MR (2007) Effects of atorvastatin on bone in postmenopausal women with dyslipidemia: a double-blind, placebo-controlled, dose-ranging trial. J Clin Endocrinol Metab 92:4671–4677
22. Huang JH, Huang XH, Chen ZY, Zheng QS, Sun RY (2004) Dose conversion among different animals and healthy volunteers in pharmacological study. Chin J Clin Pharmacol Ther 9:1069–1072
23. U.S. Food and Drug Administration (2005) FDA Guidance for industry and reviews estimating the maximum safe starting dose in initial clinical trials for therapeutics in adult healthy volunteers. Available from: http://www.fda.gov/downloads/Drugs/GuidanceUCM078932.pdf Accessed 07 May 2005
24. Lin SE, Huang JP, Wu LZ, Wu T, Cui L (2013) Prevention of osteopenia and dyslipidemia in rats after ovariectomy with combined aspirin and low-dose diethylstilbestrol. Biomed Environ Sci 26:249–257
25. Cui L, Li T, Liu Y, Li P, Xu B, Huang L, Chen Y, Liu Y, Tian X, Jee WS, Wu T (2012) Salvianolic acid B prevents bone loss in prednisone-treated rats through stimulation of osteogenesis and bone marrow angiogenesis. PLoS One 7:e34647
26. Lin SE, Huang JP, Zheng L, Liu YZ, Liu GH, Li N, Wang KX, Zou LY, Wu T, Qin L, Cui L, Li G (2014) Glucocorticoid-induced osteoporosis in growing rats. Calcif Tissue Int 95:362–373
27. Dempster DW, Compston JE, Drezner MK, Glorieux FH, Kanis JA, Malluche H, Meunier PJ, Ott SM, Recker RR, Parfitt AM (2013) Standardized nomenclature, symbols, and units for bone histomorphometry: a 2012 update of the report of the ASBMR Histomorphometry Nomenclature Committee. J Bone Miner Res 28:2–17
28. Campbell GM, Bernhardt R, Scharnweber D, Boyd SK (2011) The bone architecture is enhanced with combined PTH and alendronate treatment compared to monotherapy while maintaining the state of surface mineralization in the OVX rat. Bone 49:225–232
29. Mahanti HS, Barnes RM (1983) Determination of major, minor and trace elements in bone by inductively-coupled plasma emission spectrometry. Anal Chim Acta 151:409–417
30. Little Tanya J, Feinle-Bisset Christine (2010) Oral and gastrointestinal sensing of dietary fat and appetite regulation in humans: modification by diet and obesity. Front Neurosci 4:178
31. Paquette A, Shinoda M, Rabasa Lhoret R, Prud'homme D, Lavoie JM (2007) Time course of liver lipid infiltration in ovariectomized rats: impact of a high-fat diet. Maturitas 58:182–190
32. Grundy SM, Cleeman JI, Merz CN, Brewer HB Jr, Clark LT, Hunninghake DB, Pasternak RC, Smith SC Jr, Stone NJ (2004) Implications of recent clinical trials for the National Cholesterol Education Program Adult Treatment Panel III guidelines. Circulation 110:227–239
33. Expert Panel on Detection, Evaluation, and Treatment of High Blood Cholesterol in Adults (2001) Executive summary of the third report of the National Cholesterol Education Program (NCEP) Expert panel on Detection Evaluation and Treatment of High Blood Cholesterol in Adults (Adult Treatment Panel III). JAMA 285:2486–2497
34. Stein EA (2003) The power of statins: aggressive lipid lowering. Clin Cardiol 26:III25–III31
35. Parhami F, Tintut Y, Beamer WG, Gharavi N, Goodman W, Demer LL (2001) Atherogenic high-fat diet reduces bone mineralization in mice. J Bone Miner Res 16:182–188
36. Cao JJ, Gregoire BR, Gao H (2009) High-fat diet decreases cancellous bone mass but has no effect on cortical bone mass in the tibia in mice. Bone 44:1097–1104
37. Patsch JM, Kiefer FW, Varga P, Pail P, Rauner M, Stupphann D, Resch H, Moser D, Zysset PK, Stulnig TM, Pietschmann P (2011) Increased bone resorption and impaired bone microarchitecture in short-term and extended high-fat diet-induced obesity. Metabolism 60:243–249
38. Seeman E, Delmas PD (2006) Bone quality–the material and structural basis of bone strength and fragility. N Engl J Med 354:2250–2261
39. Kaji H, Kanatani M, Sugimoto T, Chihara K (2005) Statins modulate the levels of osteoprotegerin/receptor activator of NFκB ligand mRNA in mouse bonecell cultures. Horm Metab Res 37:589–592
40. Viereck V, Grundker C, Blaschke S, Frosch KH, Schoppet M, Emons G, Hofbauer LC (2005) Atorvastatin stimulates the production of osteoprotegerin by human osteoblasts. J Cell Biochem 96:1244–1253